Enhancing CRISPR deletion via pharmacological delay of DNA-PK

Núria Bosch (1,2,4),

Michaela Medová (2,3),

Roberta Esposito (1,2),

Carlos Pulido-Quetglas (1,2,4)

Yitzhak Zimmer (2,3),

Rory Johnson* (1,2)

1. Department of Medical Oncology, Inselspital, Bern University Hospital, University of Bern, Switzerland

2. Department for BioMedical Research, University of Bern, Bern, Switzerland

3. Department of Radiation Oncology, Inselspital, Bern University Hospital, University of Bern, Switzerland

4. Graduate School of Cellular and Biomedical Sciences, University of Bern, Bern, Switzerland

*Correspondence: rory.johnson@dbmr.unibe.ch

Abstract

CRISPR-Cas9 deletion (CRISPR-del) is the leading approach for eliminating DNA from mammalian cells and underpins a variety of genome-editing applications. Target DNA, defined by a pair of double strand breaks (DSBs), is removed during non-homologous end-joining (NHEJ). However, the low efficiency of CRISPR-del results in laborious experiments and false negative results. Using an endogenous reporter system, we demonstrate that temporary inhibition of DNA-dependent protein kinase (DNA-PK) – an early step in NHEJ - yields up to 17-fold increase in DNA deletion. This is observed across diverse cell lines, gene delivery methods, commercial inhibitors and guide RNAs, including those that otherwise display negligible activity. Importantly, the method is compatible with pooled functional screens employing lentivirally-delivered guide RNAs. Thus, delaying the kinetics of NHEJ relative to DSB formation is a simple and effective means of enhancing CRISPR-deletion.

Keywords: CRISPR; CRISPR deletion ; DNA-PK ; genome editing ; reporter assay; DNA.

Introduction

CRISPR-Cas9 technology enables a variety of loss-of-function perturbations to study the functions of genomic elements in their natural context, and engineer natural and unnatural mutations (Cong et al. 2013; Mali et al. 2013; Doench 2017). One such application, CRISPR-deletion (CRISPR-del), is a means of permanently removing specific genomic fragments from 10^1 – 10^6 base pairs (Canver et al. 2014). This range has enabled researchers to investigate a wide variety of functional elements, including gene regulatory sequences (Canver et al. 2015; Mochizuki et al. 2018; Gasperini et al. 2019), non-coding RNAs (Han et al. 2014; Ho et al. 2015; Holdt et al. 2016; Koirala et al. 2017; Xing et al. 2017), and structural elements (Huang et al. 2018). Similarly, engineered deletions can be used to model human mutations (Lupiañez et al. 2015; Nelson et al. 2016). CRISPR-del is readily scaled to high throughput screens, via pooled lentiviral libraries of thousands of paired single guide RNAs (sgRNAs) (Vidigal and Ventura 2015; Aparicio-Prat et al. 2015).

This has been used to discover long noncoding RNAs (lncRNAs) regulating cancer cell proliferation (Zhu et al. 2016; Liu et al. 2018) and to map *cis*-regulatory regions of key protein-coding genes (Gasperini et al. 2017; Diao et al. 2017).

CRISPR-del employs a pair of CRISPR-Cas9 complexes to introduce double strand breaks (DSBs) at two sites flanking the target region. Thereafter it relies on the endogenous non-homologous end joining (NHEJ) process to repair the breaks so as to eject the intervening fragment (Yang et al. 2013; Maddalo et al. 2014; Ho et al. 2015; Vidigal and Ventura 2015). The two ends of target regions are defined by a pair of user-designed sgRNAs (Pulido-Quetglas et al. 2017). Paired sgRNAs may be delivered by transfection or viral transduction (Vidigal and Ventura 2015; Aparicio-Prat et al. 2015). Pooled screens require that both sgRNAs are encoded in a single vector to ensure their simultaneous delivery, and are typically performed under conditions of low multiplicity-of-infection (MOI), where each cell carries a single lentiviral insertion (Vidigal and Ventura 2015; Zhu et al. 2016; Gasperini et al. 2017; Esposito et al. 2019; Doench 2018).

The principal drawback of CRISPR-del is the low efficiency with which targeted alleles are deleted. Studies on cultured cells typically report efficiencies in the range 0% – 50% of alleles, and often <20% (Mandal et al. 2014; Thomas et al. 2020), similar to estimates from individual clones (Canver et al. 2014; Vidigal and Ventura 2015; Aparicio-Prat et al. 2015; Ho et al. 2015; Pulido-Quetglas et al. 2017). Indeed, a recent publication reported high variation in the efficiencies of paired sgRNA targeting the same region, including many that yielded negligible deletion (Thomas et al. 2020). Transfection typically yields greater efficiency than viral transduction, possibly due to higher sgRNA levels (Mangeot et al. 2019), but is incompatible with pooled screening. Although megabase-scale deletions have been reported (Han et al. 2014; Essletzbichler et al. 2014), deletion efficiency decreases with increasing target size (Canver et al. 2014). Homozygous knockout clones may be isolated by screening hundreds of single cells, however this is slow and laborious, and resulting clones may not be representative of the general population (Stojic et al. 2018). More important than these practical costs, is the potential impact of low deletion rates on the ability to discern *bona fide* functional effects arising from a given mutation (Thomas et al. 2020). Non-performing sgRNA pairs are a particular problem for pooled CRISPR-del screens, where they reduce statistical power and lead to false negative results. In the screen reported by Zhu at al,.less than half of pgRNAs yielded a detectable phenotype, strongly suggesting they do not efficiently delete their targets (Fig. 1A) (Zhu et al. 2016). Similar results are

reported by Canver et al, where 65% of pgRNAs yielded deletion efficiency <20% (Canver et al. 2014). There is no observable correlation between phenotype and average predicted score of the two sgRNAs (Fig. 1B) (Zhu et al. 2016). This suggest that deletion efficiency of a given pgRNA does not simply depend on the aggregate quality of its two individual sgRNAs. The outcome is that researchers are forced to increase the coverage of deletion constructs per target, resulting in lower candidate numbers and increased costs (Doench et al. 2016; Sanson et al. 2018). Consequently, any method to improve CRISPR-del efficiency would streamline experiments and enable the discovery of presently-overlooked functional elements.

For other applications of CRISPR, most notably precise genome editing using homologous recombination (HR), substantial gains have been made editing efficiency (Yeh et al. 2019). Here, editing events are rare, and HR is the rate-limiting-step (Mao et al. 2008; Miyaoka et al. 2016). The two principal strategies to boost efficiency are: (1) direct stimulation of homology directed repair (HDR) (Riesenberg and Maricic 2018; Yeh et al. 2019; Song et al. 2016; Lin et al. 2014); (2) suppression of the competing NHEJ pathway at early stages through inhibition of Ku70/80 complex (Fattah et al. 2008; Riesenberg and Maricic 2018; Yeh et al. 2019) or DNA-dependent protein kinase (DNA-PK) (Robert et al. 2015; Riesenberg and Maricic 2018; Riesenberg et al. 2019; Yeh et al. 2019), or at late phases, via Ligase IV (LigIV) inhibition (Chu et al. 2015; Maruyama et al. 2015; Riesenberg and Maricic 2018; Yeh et al. 2019). To date, however, there are no reported methods for pharmacological enhancement of CRISPR-del.

Towards this aim, we consider the events necessary for successful deletion (Fig. 1C). In the presence of two DSBs, NHEJ gives rise to successful deletion. For this to occur, the DSBs must occur on a timescale shorter than that required for NHEJ. Otherwise, the first DSB is repaired by NHEJ *before* the second can occur, and deletion will not take place. Furthermore, there is a high probability that the target protospacer or protospacer adjacent motif (PAM) is mutated during NHEJ, rendering it inaccessible to the sgRNA and precluding any subsequent deletion (Canver et al. 2014).

A prediction of this model, is that successful deletion can be promoted by extending the time over which DSBs persist without being repaired, and hence increasing the likelihood that both DSBs co-occur. In other words, we hypothesise that CRISPR-del may be improved by pharmacologically slowing the rate of NHEJ during the period while DSBs are taking place. Here, we show that inhibition of DNA-PK, an early step in

NHEJ, indeed improves CRISPR-del efficiency, regardless of cell type, target region, sgRNA or inhibitory molecule, and represents a practical strategy for a variety of applications including pooled library screening.

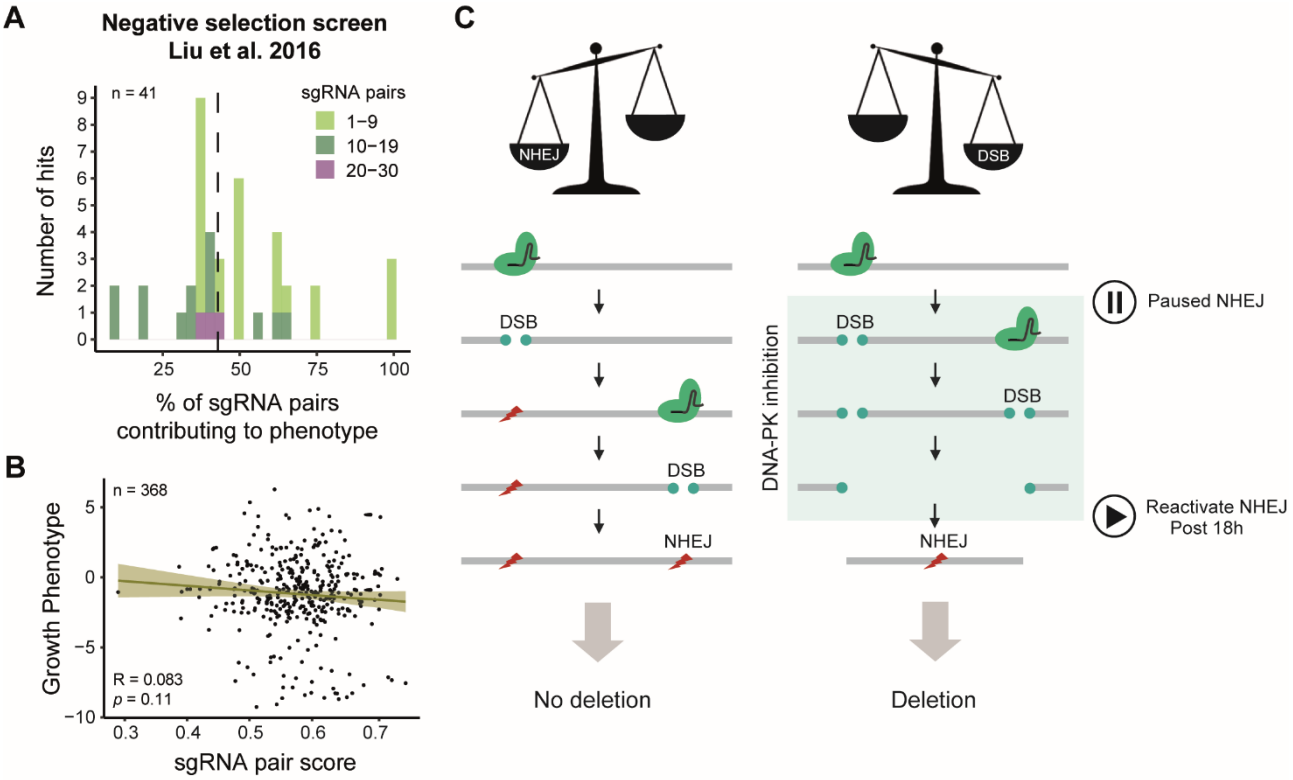

Figure 1. Analysis of sgRNA pairs efficiencies from public data and CRISPR-deletion model. (A, B), Re-analysis of the hits obtained CRISPR-del negative selection screen in Huh.7 cells from Zhu et al. 2016 (excluding hits targeting ORFs). (A) The upper histogram shows the percentage of sgRNA pairs contributing to the phenotype of each hit (x axis) versus the number of hits included in each bin (y axis). The dashed line represents the median (42.86%). Hits have been divided in three groups by the total number of sgRNAs designed (light green, dark green and purple). (B) The scatter plot represents the mean of the individual sgRNAs scores within a pair (calculated with the Rule Set II algorithm from Doench et al. 2016) versus the Log2 Fold Change (Growth Phenotype) obtained by Zhu et al. 2016. Pearson correlation (R) and *p*-value (*p*) are shown. (C) Model for CRISPR-del and its improvement by inhibition of DNA-PK.

Results

A quantitative endogenous reporter for CRISPR-del

To identify factors capable of improving CRISPR-del efficiency, we designed a gene-based reporter system: CRISPR Deletion Endogenous Reporter (CiDER). Such a system should be quantitative, sensitive, practical and able to closely model the CRISPR-del process by targeting endogenous genes rather than plasmids. We

117 focussed on genes encoding cell-surface proteins, as they can be rapidly and sensitively detected by flow
118 cytometry (Bausch-Fluck et al. 2015). A number of candidates were considered with criteria of (1) non-
119 essentiality for cell viability and proliferation (Luo et al. 2008; Meyers et al. 2017; Tsherniak et al. 2017)
120 (https://depmap.org), (2) high expression in human cell lines (Thul et al. 2017) (http://www.proteinatlas.org),
121 (3) lack of overlap with other genomic elements that could lead to false positive detection, and (4) availability
122 of flow-cytometry grade antibody. Consequently, we selected *PLXND1* encoding the Plexin-D1 protein
123 (Supplementary Fig. 1), which presents three genomic copies in HeLa cells and two in HCT116 cells
124 according to the Cancer Cell Line Enciclopedia (CCLE) (Barretina et al. 2012)
125 (https://portals.broadinstitute.org/ccle/data).

126 We conceived an experimental setup where only successful CRISPR-del leads to loss of *PLXND1* expression,
127 but unsuccessful events do not. In this scheme, the gene's first exon is targeted for deletion by a series of
128 sgRNA pairs recognising the non-protein coding regions upstream (promoter) and downstream (first intron)
129 (Fig. 2A). Successful deletions of the first exon are expected to silence protein expression, but indels from
130 individual sgRNAs do not affect the protein sequence directly and should not lead to silencing. Finally, we
131 also designed sgRNAs that directly target the open reading frame (ORF), since these are expected to yield
132 maximal protein silencing (designated positive control, *P+*).

133 We used flow cytometry to evaluate Plexin-D1 protein levels (Fig. 2B). Positive control sgRNAs (*P+*)
134 yielded approximately 90% knockout efficiency. We observed wide variability in the deletion efficiency of
135 sgRNA pairs, from Pair1 (*P1*) displaying minimal efficacy, to the most efficient *P4* yielding ~40% deletion.
136 Therefore these paired sgRNAs achieve deletion efficiencies that are comparable to previous studies (Canver
137 et al. 2014; Pulido-Quetglas et al. 2017). Measured deletion rates were consistent across biological replicates
138 (Fig. 2B). The observed loss of Plexin-D1 was not due to large indels or disruption of gene regulatory
139 elements at individual sgRNA target sites (Kosicki et al. 2018), since control experiments with single
140 sgRNAs showed no loss of Plexin-D1 (Supplementary Fig. 2). In CiDER we have a reproducible and
141 practical reporter of CRISPR-del at a range of efficiencies.

142

143

Temporary inhibition of DNA-PK during DSB formation increases CRISPR-del efficiency

We hypothesized that temporarily inhibiting NHEJ during DSB formation would favour CRISPR-del, by increasing the chance that both DSBs will co-occur (Fig. 1C). We tested DNA-PK, a DNA end-binding factor at the first step of NHEJ pathway, for which a number of small-molecule inhibitors are available (Harnor et al. 2017). We began by treating HeLa cells with the inhibitor M3814 (IC_{50}=3nM) (Fuchss et al. 2014; Zenke et al. 2016; Riesenberg et al. 2019) at two concentrations (300 nM and 900 nM). Importantly, cells constitutively expressing Cas9 were treated for an 18 hour time window, 4 hours after sgRNA expression plasmid delivery by transfection. Thus, DNA-PK was inhibited immediately before sgRNA expression. This resulted in improved deletion rates for all four sgRNA pairs, including a 17-fold increase for *P1,* which otherwise displays negligible deletion under normal conditions (Fig. 2C,E).

We next asked whether other inhibitors of DNA-PK yield a similar effect. We treated cells with four other commercially-available molecules at a concentration of 10uM: KU57788 (IC_{50}=14nM), NU7026 (IC_{50}=230nM), LTURM34 (IC_{50}=34nM) and DMNB (IC_{50}=15uM) (Fig. 2F). Each one yielded increases in CRISPR-del efficiency to varying degrees, correlating with published differences on the inhibition potency (Mohiuddin and Kang 2019). As expected based on previous literature, KU57788 gave the strongest effect (Mohiuddin and Kang 2019) and DMNB gave the weakest effect, likely due to its high IC_{50}.

We were curious whether improved deletion depends on inhibition specifically of DNA-PK, or more generally on NHEJ. To answer this, we used SCR7 pyrazine to inhibit another step in NHEJ, the final ligation by Ligase IV (LigIV). In contrast to DNA-PK, this treatment did not improve deletion efficiency (Fig. 3A). At this late stage, the NHEJ machinery (DNA-end binding and processing complex) is already maintaining together the free DNA ends. When LigIV activity is restored, it may be more likely that each single DSB is repaired independently, introducing small indels rather than favouring genomic deletion. Thus, CRISPR-del efficiency improvements depend specifically on inhibition of DNA-PK activity. Altogether, we have shown that pharmacological inhibition of NHEJ at the DNA-PK step yields enhanced deletion of *PLXND1* reporter in HeLa cells.

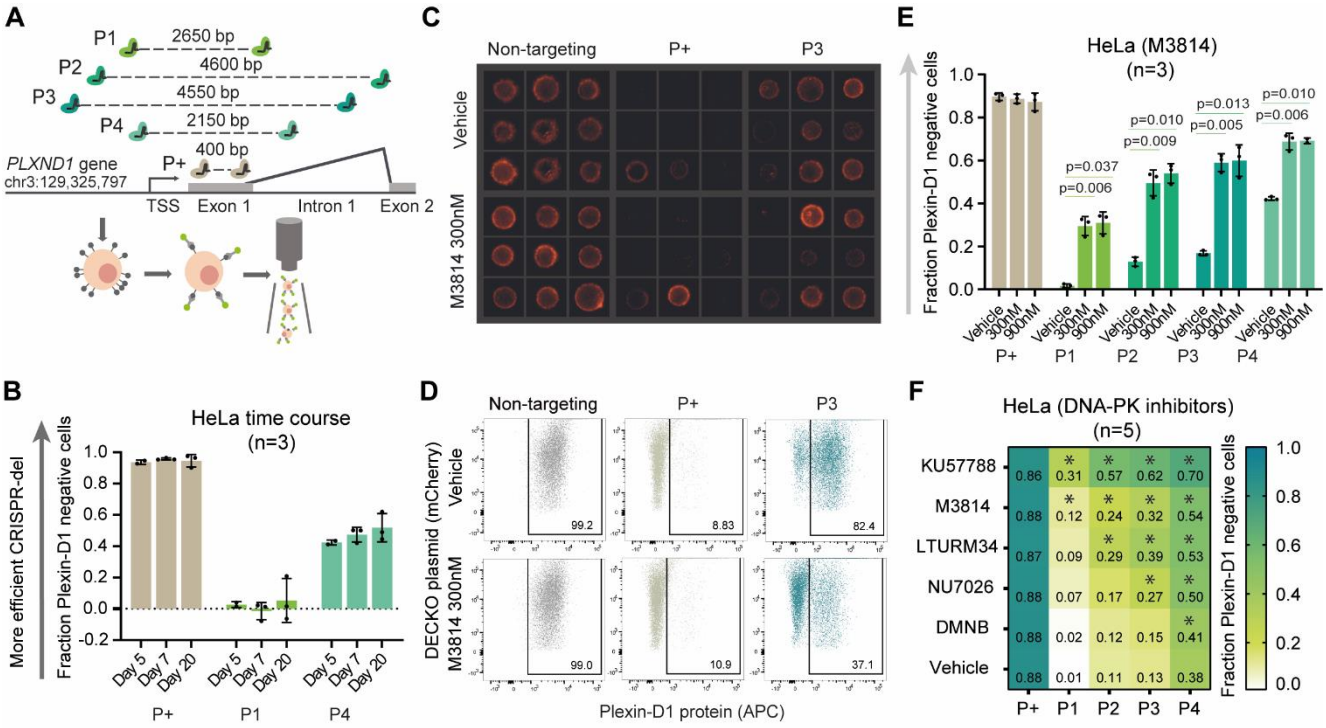

Figure 2. CiDER reporter system identifies DNA-PK inhibition as a means to increase CRISPR-del efficiency. (A) The CiDER endogenous reporter relies on a series of sgRNA pairs targeting exon 1 of *PLXND1* locus, whose protein product is read out by flow cytometry. (B) CRISPR-del efficiency time course in HeLa (mean, standard deviation). (C) Representative images of Plexin-D1 (APC) staining in HeLa. (D) Representative raw flow cytometry plots of CiDER in HeLa upon DNA-PK inhibition. Plexin-D1 positive cells are gated and numbers correspond to percentage of cells. (E) CRISPR-del efficiency of CiDER in HeLa upon DNA-PK inhibition (mean, standard deviation, 2-tailed paired *t*-test). (F) CRISPR-del efficiency of CiDER in HeLa upon DNA-PK inhibition with different small molecules (mean and 2-tailed paired *t*-test).

Generality of deletion enhancement by DNA-PK inhibition

We next assessed whether this DNA-PK-inhibition is more generally effective across cell lines, genomic targets and sgRNA delivery modalities.

We began by replicating CiDER experiments in two widely-used cell lines, HCT116 and HEK293T (Thomas et al. 2020; Li and Richard 2016; Hart et al. 2015; Liu et al. 2017) (Fig. 3B). Both have baseline CRISPR-del efficiency below HeLa, possibly due to weaker NHEJ activity (Miyaoka et al. 2016). Nevertheless, DNA-PK inhibition enhanced deletion in both cell backgrounds.

All experiments so far involved a single target locus, assayed by flow cytometry. We next assessed whether these effects hold for other loci and readouts. We previously used a quantitative PCR method (quantitative CRISPR PCR, QC-PCR) to measure rates of deletion at the *MALAT1* enhancer region (Pulido-Quetglas et

al. 2017). For three out of four sgRNA pairs, we observed a significant enhancement of deletion with M3814 treatment of HeLa (Fig. 3C, note the inverted scale used for QC-PCR). Similar but weaker results were also observed for HCT116 (two out of four pairs) and HEK293T cells (one out of four pairs) (Supplementary Fig. 3).

Together, although differences in performance are observed between cell types, these findings support the general applicability of DNA-PK inhibition.

DNA-PK inhibition in the context of high-throughput pooled screens

CRISPR-del perturbations can be employed in the context of pooled functional screens, where libraries of paired sgRNAs are delivered by lentivirus at low MOI, and the effect on phenotypes such as proliferation are recorded. We asked whether DNA-PK inhibition is also practical under these conditions, by targeting the *PLXND1* reporter with sgRNAs delivered by low-MOI lentivirus. In initial experiments, M3814 was added to cell media prior to lentiviral transduction, but no improvement in deletion efficiency was observed (data not shown). This is explained by the fact that lentiviruses require NHEJ for genomic integration (Li et al. 2001; Rene et al. 2004). Therefore, we modified our protocol so as to leave sufficient time for viral integration before NHEJ inhibition (24 h was optimal, Supplementary Fig. 4), and observed a 2.7-fold increase in CRISPR-del efficiency (Fig. 3D).

Pooled CRISPR screens employ phenotypic readouts, often in the form of cell proliferation (Esposito et al. 2019; Doench 2017). To test whether improved CRISPR-del translates into stronger phenotypes, we developed a reporter assay capable of quantifying the phenotypic effect of CRISPR-del in terms of cell death. Analagous to *PLXND1* (Fig. 2A), we designed three pairs of sgRNAs targeting the first exon of the essential gene, *RPS5* (coding for the 40S ribosomal protein S5, P46782, Uniprot): *RPS5-P+*, *P9*, *P10*, *P11*. As expected, sgRNAs targeting the *AAVS1* locus had no effect, while sgRNAs targeting the RPS5 ORF (*RPS5-P+*) resulted in ~47% mortality after 72 h (Fig. 3E). Neither was affected by M3814, indicating no detectable toxicity at this working concentration, as also shown by Riesenberg et al (Riesenberg et al. 2019). In contrast, three pairs of sgRNAs targeting the first exon of *RPS5* (*P9*, *P10*, *P11*) resulted in a substantial mortality

(32%, 21% and 15%, respectively), which was significantly enhanced by addition of M3814 (41%, 30% and 22%, respectively).

In conclusion, DNA-PK inhibition enhances CRISPR-del when sgRNAs are delivered lentivirally at low MOI, and results in increased downstream phenotypic effects, supporting its utility in the context of high-throughput pooled screens.

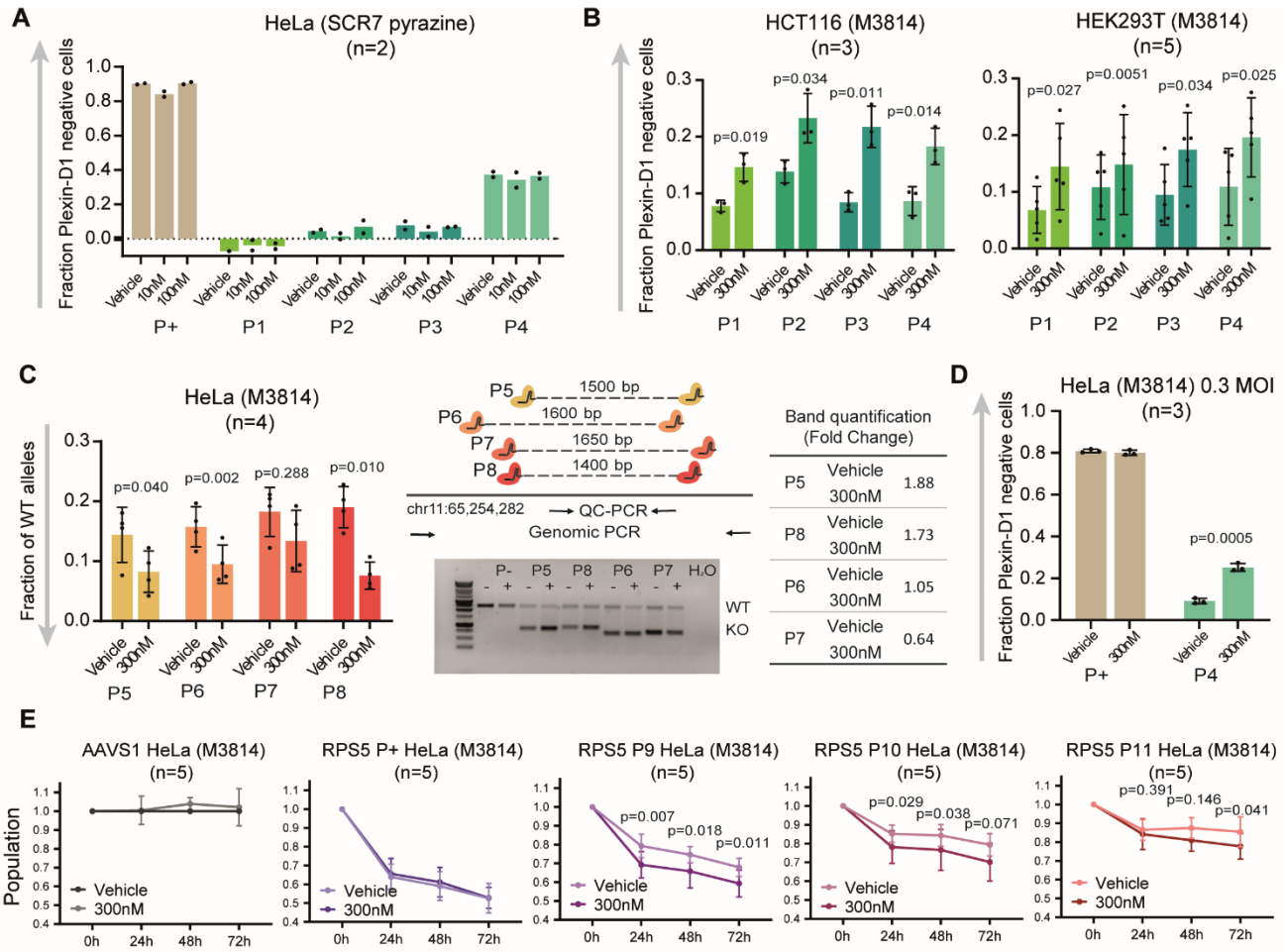

Figure 3. Universality of DNA-PK inhibition. (A) CRISPR-del efficiency of CiDER in HeLa upon LigIV inhibition (mean). (B) CRISPR-del efficiency of CiDER in HCT116 and HEK293T cell lines upon DNA-PK inhibition (mean, standard deviation, 2-tailed paired *t*-test). (C) CRISPR-del efficiency in chr11-locus in HeLa upon DNA-PK inhibition. The bar plots show the fraction of WT allele quantified by qPCR (mean, standard deviation, 2-tailed paired *t*-test). Shown a scheme of the sgRNA pairs and PCR primers design for this locus. Also shown a representative agarose gel from the genomic PCR of the region and band quantification of the KO allele. (D) CRISPR-del efficiency of CiDER in HeLa upon low MOI lentiviral infection and DNA-PK inhibition (mean, standard deviation, 2-tailed paired *t*-test). (E) Functional validation of DNA-PK inhibition. Viability assays after RPS5 TSS deletion upon DNA-PK inhibition (mean, standard deviation, 2-tailed paired *t*-test).

Discussion

The intrinsic DNA damage response underpins CRISPR-Cas9 genome editing and may be manipulated to favour desired editing outcomes. In the case of precise genome editing, which is based on the HDR pathway, efficiency has been substantially improved through pharmacological promotion of HDR and inhibition of the competing NHEJ pathway (Yeh et al. 2019). No such solutions have been developed for CRISPR-del, despite its being one of the most common CRISPR-Cas9 modalities, with diverse scientific and technological applications (Mochizuki et al. 2018; Holdt et al. 2016; Gasperini et al. 2019; Han et al. 2014; Ho et al. 2015; Canver et al. 2015; Koirala et al. 2017; Xing et al. 2017; Huang et al. 2018; Lupiañez et al. 2015; Nelson et al. 2016).

We hypothesised that successful CRISPR-del requires paired DSBs to co-occur *before* NHEJ has time to act, and thus may be enhanced by pharmacological inhibition of DNA-PK. This is initially counter-intuitive, as DNA-PK is a necessary step in the NHEJ pathway upon which CRISPR-del relies, and its inhibition is widely used to promote HDR(Yeh et al. 2019; Riesenberg and Maricic 2018; Riesenberg et al. 2019; Robert et al. 2015). However, rather than permanently blocking NHEJ, our protocol slows the kinetics of NHEJ for a defined period while DSBs are taking place. This produces a significant enhancement of DNA deletion efficiency, increasing protein knockout rates and resulting in stronger functional effects.

DNA-PK inhibition represents a practical option for a variety of CRISPR-del applications, from basic research to gene therapy. DNA-PK inhibitors are cheap and widely-available. Deletion efficiency improved regardless of the inhibitor molecule, target region, sgRNA sequence, cell background and delivery method. Particularly striking was the observation that some sgRNA pairs that are ineffective under normal conditions, achieved respectable rates of deletion using DNA-PK inhibition. This suggests that the failure of many sgRNA pairs to efficiently delete DNA may arise not from their inability to promote DSBs, but rather as a result of poor kinetic properties (for example, a mismatch in kinetics between the two individual sgRNAs). Finally, this method (with minor modifications) is compatible with low-MOI lentiviral delivery and leads to improvements in observed cell phenotypes. These conditions are employed in pooled screens to probe the functions of non-protein coding genomic elements (Zhu et al. 2016; Gasperini et al. 2017; Diao et al. 2017; Liu et al. 2018), meaning that DNA-PK inhibition may be used in future to improve the sensitivity of

CRISPR-deletion screens by boosting the number of active sgRNA pairs, and their efficiency. This study focussed on genetic delivery methods and transformed cell types that are commonly used in high-throughput screens. Nevertheless, it will be important to assess in future the performance of DNA-PK inhibition with Cas9 ribonucleoprotein (RNP) delivery methods and in primary and non-transformed cellular backgrounds.

Materials and methods

Cell culture. HeLa, HCT116 and HEK293T were cultured on Dulbecco's Modified Eagles Medium (DMEM) (Sigma-Aldrich, D5671) supplemented with 10% Fetal Bovine Serum (FBS) (ThermoFisher Scientific, 10500064), 1% L-Glutamine (ThermoFisher Scientific, 25030024), 1% Penicillin-Streptomycin (ThermoFisher Scientific, 15140122). Cells were grown at 37°C and 5% CO_2 and passaged every two days at 1:5 dilution.

Generation of Cas9 stable cell lines. HeLa cells were infected with lentivirus carrying the Cas9-BFP (blue fluorescent protein) vector (Addgene 52962). HCT116 and HEK293T were transfected with the same vector using Lipofectamine 2000 (ThermoFisher Scientific, 11668019). All cell types were selected with blasticidin (4ug/ml) for at least five days and selected for BFP-positive cells twice by fluorescence activated cell sorting.

sgRNA pair design and cloning. sgRNA pairs were designed using CRISPETa (http://crispeta.crg.eu/) and cloned into the pDECKO backbone as described previously (Pulido-Quetglas et al. 2017). Off-target filters did not allow less than 3 mismatches for each sgRNA sequence. No positive or negative masks were applied in the search. Minimum individual score was set at 0.2 and minimum paired score at 0.4. The sgRNA pairs were then manually selected from the output list. All sgRNA sequences may be found in Supplementary Figure 5.

Inhibitors. All molecules used in this study are commercially available: M3814 (MedChemExpress, HY-101570), KU57788 (MedChemExpress, HY-11006), NU7026 (MedChemExpress, HY-15719), LTURM34

(MedChemExpress, HY-101667), DMNB (ToChris, 2088) and SCR7 Pyrazine (Sigma-Aldrich, SML1546). 10mM stocks (and 5mM for NU7026, due to solubility limitations) were prepared by resuspension in dimethylsulfoxide (DMSO) (Sigma-Aldrich, D4540).

Transfection and lentiviral transduction. For transfection experiments, 70% confluent 12-well plates were transfected using Lipofectamine 2000 (ThermoFisher Scientific, 11668019) with 1250 ng of pDECKO plasmid following provider's guidelines. After 6 hours, transfection media was replaced for fresh complete DMEM (10% FBS, 1% L-Glutamine and 1% Penicillin-Streptomycin) and the corresponding small molecule was added to media for 18 hours. The treatment was finished by replacing the media with complete DMEM. After one day cells were selected with puromycin (2ug/ml).

For lentiviral infection experiments, cells were spin-infected at a 0.3 multiplicity of infection in the presence of DMEM (10% FBS, 1% L-Glutamine) and hexadimethrine bromide (8ug/ml) (Sigma-Aldrich, 107689) at 2000 rpm, 37°C during 1.5 hours. After 0, 5, 10, 24, 48, 72 hours, infection media was replaced for fresh complete DMEM (10% FBS, 1% L-Glutamine and 1% Penicillin-Streptomycin) and the corresponding small molecule was added to media for 18 hours. The treatment was finished by replacing the media with complete DMEM and puromycin (2ug/ml) to start the selection.

Flow cytometry. After five days of puromycin selection, cells were trypsinized, resuspended in PBS and incubated for 30 minutes at room temperature (RT) with the human α-PlexinD1 mouse monoclonal antibody (1:150 dilution) (R&D systems, MAB4160). Cells were washed twice with PBS and incubated for 30 minutes at RT with an α-Mouse IgG secondary goat antibody conjugated to the APC fluorochrome (1:200 dilution) (eBioscience, 17-4010-82). Cells were washed and resuspended in PBS, processed with the LSRII SORP flow cytometer and analysed with FlowJo_v10 software. A total of 10,000 cells per sample are sorted. Cell population is selected in the SSC-A/FSC-A plot. Single cells are gated in the FSC-H/FSC-A plot. Finally, the APC positive population is set in the mCherry/APC plot in the control sample and expanded to all the other samples without modification. The fraction of Plexin-D1 negative singlet cells is calculated by gating Plexin-D1 positive singlet cells, normalizing to a non-targeting control and subtracting the value to 1 (negative cells = 1 – positive cells). An example of the gating strategy may be found in Supplementary Figure 6.

Single cell imaging was performed using ImageStream (Luminex) and analysed with IDEAS software.

Genomic PCRs. After 5 days of puromycin selection, cells were collected and genomic DNA (qDNA) was extracted using GeneJET Genomic DNA Purification Kit (ThermoFisher Scientific, K0722). Genomic PCR was performed using GoTaq® G2 DNA Polymerase (Promega, M7841) from 10ng gDNA (Forward: *5' CCTGCTATGAACTGACCCATG 3'*, Reverse: *5' CCTGAACAGTCAGTCCATGCT 3'*)

Genomic quantitative PCRs. After 5 days of puromycin selection, cells were collected and genomic DNA (qDNA) was extracted using GeneJET Genomic DNA Purification Kit (ThermoFisher Scientific, K0722). Quantitative real time PCR (qPCR) from 10ng of gDNA was performed using GoTaq qPCR Master Mix (Promega, A6001) on a TaqMan Viia 7 Real-Time PCR System. (Target sequence - Forward: *5' GCTGGGGAATCCACAGAGAC 3'*, Reverse: *5' CATCTCAGCCCTTGTTATCCTG 3'*) and (LDHA - Forward: *5' TGGGCAGTAGAAAGTGCAG 3'*, Reverse: *5' TACCAGCTCCCACTCACAG 3'*). Target sequence primers were normalized to primers targeting the distal, non-targeted gene LDHA. Data were normalised using the ΔΔCt method (Schmittgen and Livak 2008).

Cell viability assay. CellTiter-Glo® 2.0 Cell Viability Assay (Promega, G9241) was performed upon puromycin selection (2 days post transfection). 3000 cells/well were seeded in 96-well white polystyrene plates (Corning®, Sigma-Aldrich CLS3610-48EA) and cell viability was measured in technical duplicates during 4 consecutive days (0h, 24h, 48h, 72h) according to the manufacturer's protocol. Luminescence was measured using a Tecan Reader Infinite 200.

Acknowledgements

We gratefully acknowledge administrative support from Ana Radovanovic and Silvia Roesselet (DBMR, University of Bern). We thank Bill Keyes (IGBMC) and Norbert Polacek (DCB, University of Bern) for insightful feedback and discussions. We also thank Stefan Müller (DBMR, University of Bern) for his expertise with ImageStream and the other members of the FACS lab from the University of Bern for their advice. We also acknowledge Taisia Polidori and Paulina Schaerer (DBMR, University of Bern) for the

experimental support, Álvaro Andrades (Universidad de Granada) for the CCLE data and the rest of the members of Johnson's lab for their valuable input. Andrea Maddalena (Department of Physiology, University of Bern) provided valuable advice regarding lentiviral transduction inhibition.

Funding

This work was funded by the Swiss National Science Foundation through the National Center of Competence in Research (NCCR) "RNA & Disease", by the Medical Faculty of the University and University Hospital of Bern, by the Helmut Horten Stiftung and Krebsliga Schweiz (4534-08-2018).

Author contributions

N.B. and R.J. conceived and designed the experiments. N.B. performed all the experiments and analysis of public data. M.M. and Y.Z. suggested DNA-PK inhibition to modulate NHEJ. C.P. contributed on the design of the sgRNA pairs and analysis of public data. R.E. provided the solution to circumvent lentiviral infection problems. N.B. and R.J. wrote the whole manuscript with feedback from M.M. and Y.Z. Finally, R.J. directed the research.

Data availability

The authors declare that all the data supporting the findings of this study are available within the paper and its supplementary information files.

Ethics approval and consent to participate

Not applicable.

Competing interests

The authors declare that they do not have competing interests.

355 **References**

356

357 Aparicio-Prat E, Arnan C, Sala I, Bosch N, Guigó R, Johnson R, Guigo R, Johnson R, Guigó R,
358 Johnson R, et al. 2015. DECKO: Single-oligo, dual-CRISPR deletion of genomic elements
359 including long non-coding RNAs. *BMC Genomics* **16**: 846.
360 http://bmcgenomics.biomedcentral.com/articles/10.1186/s12864-015-2086-z (Accessed March 13,
361 2018).
362 Barretina J, Caponigro G, Stransky N, Venkatesan K, Margolin AA, Kim S, Wilson CJ, Lehár J,
363 Kryukov G V., Sonkin D, et al. 2012. The Cancer Cell Line Encyclopedia enables predictive
364 modelling of anticancer drug sensitivity. *Nature* **483**: 603–607.
365 Bausch-Fluck D, Hofmann A, Bock T, Frei AP, Mirkowska P, Härtlová A, Eyk JE Van, Bourquin J.
366 2015. A Mass Spectrometric-Derived Cell Surface Protein Atlas. *PLoS One* 1–22.
367 Canver MC, Bauer DE, Dass A, Yien YY, Chung J, Masuda T, Maeda T, Paw BH, Orkin SH. 2014.
368 Characterization of genomic deletion efficiency mediated by CRISPR/Cas9 in mammalian cells. *J*
369 *Biol Chem* **289**: 21312–21324. http://www.jbc.org/lookup/doi/10.1074/jbc.M114.564625
370 (Accessed September 10, 2018).
371 Canver MC, Smith EC, Sher F, Pinello L, Sanjana NE, Shalem O, Chen DD, Schupp PG, Vinjamur DS,
372 Garcia SP, et al. 2015. BCL11A enhancer dissection by Cas9- mediated in situ saturating
373 mutagenesis. *Nature* **527**.
374 Chu VT, Weber T, Wefers B, Wurst W, Sander S, Rajewsky K, Kühn R. 2015. Increasing the efficiency
375 of homology-directed repair for CrIsPr-Cas9-induced precise gene editing in mammalian cells.
376 *Nat Biotechnol* **33**.
377 Cong L, Ran FA, Cox D, Lin S, Barretto R, Habib N, Hsu PD, Wu X, Jiang W, Marraffini LA, et al.
378 2013. Multiplex Genome Engineering Using CRISPR/Cas Systems. *Science (80-)* 819–823.
379 http://www.sciencemag.org/content/339/6121/819.full.html (Accessed March 9, 2018).
380 Diao Y, Fang R, Li B, Meng Z, Yu J, Qiu Y, Lin KC, Huang H, Liu T, Marina RJ, et al. 2017. A tiling-
381 deletion-based genetic screen for cis - regulatory element identification in mammalian cells. *Nat*
382 *Methods* **14**.
383 Doench JG. 2017. Am I ready for CRISPR? A user's guide to genetic screens. *Nat Rev Genet* **19**: 67–

384 80. http://www.ncbi.nlm.nih.gov/pubmed/29199283 (Accessed February 20, 2018).
385 Doench JG. 2018. Am I ready for CRISPR? A user's guide to genetic screens. *Nat Rev Genet* **19**: 67–
386 80. http://dx.doi.org/10.1038/nrg.2017.97.
387 Doench JG, Fusi N, Sullender M, Hegde M, Vaimberg EW, Donovan KF, Smith I, Tothova Z, Wilen C,
388 Orchard R, et al. 2016. Optimized sgRNA design to maximize activity and minimize off-target
389 effects of CRISPR-Cas9. *Nat Biotechnol* **34**: 184–191. http://www.nature.com/articles/nbt.3437
390 (Accessed September 10, 2018).
391 Esposito R, Bosch N, Lanzós A, Polidori T, Pulido-Quetglas C, Johnson R. 2019. Hacking the Cancer
392 Genome: Profiling Therapeutically Actionable Long Non-coding RNAs Using CRISPR-Cas9
393 Screening. *Cancer Cell* **35**: 545–557.
394 Essletzbichler P, Konopka T, Santoro F, Chen D, Gapp B V, Kralovics R, Brummelkamp TR, Nijman
395 SMB. 2014. Megabase-scale deletion using CRISPR / Cas9 to generate a fully haploid human cell
396 line. *Genome Res* **24**: 2059–2065.
397 Fattah FJ, Lichter NF, Fattah KR, Oh S, Hendrickson EA. 2008. Ku70 , an essential gene , modulates
398 the frequency of rAAV-mediated gene targeting in human somatic cells. *PNAS* **105**: 8703–8708.
399 Fuchss T, Emde U, Buchstaller H-P, W.K.R. WM. 2014. WO2014183850A1.
400 Gasperini M, Findlay GM, McKenna A, Milbank JH, Lee C, Zhang MD, Cusanovich DA, Shendure J.
401 2017. CRISPR/Cas9-Mediated Scanning for Regulatory Elements Required for HPRT1
402 Expression via Thousands of Large, Programmed Genomic Deletions. *Am J Hum Genet*.
403 http://www.sciencedirect.com/science/article/pii/S0002929717302458 (Accessed July 18, 2017).
404 Gasperini M, Hill AJ, Trapnell C, Ahituv N, Martin B, Kim S, Zhang MD, Jackson D, Leith A,
405 Schreiber J, et al. 2019. A Genome-wide Framework for Mapping Gene Regulation via Cellular
406 Genetic Screens. *Cell* **176**: 377–390.
407 Han J, Zhang J, Chen L, Shen B, Zhou J, Hu B, Du Y, Tate PH, Huang X, Zhang W. 2014. Efficient in
408 vivo deletion of a large imprinted lncRNA by CRISPR/Cas9. *RNA Biol* **11**: 829–35.
409 http://www.ncbi.nlm.nih.gov/pubmed/25137067 (Accessed May 11, 2017).
410 Harnor SJ, Brennan A, Cano C. 2017. Targeting DNA-Dependent Protein Kinase for Cancer Therapy.
411 *ChemMedChem* **12**: 895–900.
412 Hart T, Chandrashekhar M, Aregger M, Durocher D, Steinhart Z, Brown KR, Macleod G, Mis M,

413 Zimmermann M, Fradet-Turcotte A, et al. 2015. High-Resolution CRISPR Screens Reveal Fitness
414 Genes and Genotype-Specific Cancer Liabilities. http://dx.doi.org/10.1016/j.cell.2015.11.015
415 (Accessed March 19, 2018).
416 Ho T-T, Zhou N, Huang J, Koirala P, Xu M, Fung R, Wu F, Mo Y-Y. 2015. Targeting non-coding
417 RNAs with the CRISPR/Cas9 system in human cell lines. *Nucleic Acids Res* **43**: e17.
418 http://academic.oup.com/nar/article/43/3/e17/2410995/Targeting-noncoding-RNAs-with-the-
419 CRISPRCas9 (Accessed September 10, 2018).
420 Holdt LM, Stahringer A, Sass K, Pichler G, Kulak NA, Wilfert W, Kohlmaier A, Herbst A, Northoff
421 BH, Nicolaou A, et al. 2016. Circular non-coding RNA ANRIL modulates ribosomal RNA
422 maturation and atherosclerosis in humans. *Nat Commun* **7**.
423 Huang J, Li K, Cai W, Liu X, Zhang Y, Orkin SH, Xu J, Yuan G. 2018. Dissecting super-enhancer
424 hierarchy based on chromatin interactions. *Nat Commun* **9**.
425 Koirala P, Huang J, Ho T-T, Wu F, Ding X, Mo Y-Y. 2017. LncRNA AK023948 is a positive regulator
426 of AKT. *Nat Commun* **8**: 14422. http://www.nature.com/doifinder/10.1038/ncomms14422
427 (Accessed March 28, 2018).
428 Kosicki M, Tomberg K, Bradley A. 2018. Repair of double-strand breaks induced by CRISPR – Cas9
429 leads to large deletions and complex rearrangements. *Nat Biotechnol* **36**.
430 Li L, Olvera JM, Yoder KE, Mitchell RS, Butler SL, Lieber M, Martin SL, Bushman FD. 2001. Role of
431 the non-homologous DNA end joining pathway in the early steps of retroviral infection. *EMBO J*
432 **20**.
433 Li N, Richard S. 2016. Sam68 functions as a transcriptional coactivator of the p53 tumor suppressor.
434 *Nucleic Acids Res* 1–16.
435 Lin S, Staahl BT, Alla RK, Doudna JA. 2014. Enhanced homology-directed human genome engineering
436 by controlled timing of CRISPR / Cas9 delivery. *Elife* 1–13.
437 Liu SJ, Horlbeck MA, Cho SW, Birk HS, Malatesta M, He D, Attenello FJ, Villalta JE, Cho MY, Chen
438 Y, et al. 2017. CRISPRi-based genome-scale identification of functional long noncoding RNA loci
439 in human cells. *Science (80-)* **355**: eaah7111.
440 http://www.sciencemag.org/lookup/doi/10.1126/science.aah7111 (Accessed April 25, 2017).
441 Liu Y, Cao Z, Wang Y, Guo Y, Xu P, Yuan P, Liu Z. 2018. Genome-wide screening for functional long

noncoding RNAs in human cells by Cas9 targeting of splice sites. *Nat Biotechnol* **36**.

Luo B, Cheung HW, Subramanian A, Sharifnia T, Okamoto M, Yang X, Hinkle G, Boehm JS, Beroukhim R, Weir BA, et al. 2008. Highly parallel identification of essential genes in cancer cells. *PNAS* **105**: 20380–5. http://www.pnas.org/content/105/51/20380.full (Accessed December 5, 2015).

Lupiañez DG, Kraft K, Heinrich V, Krawitz P, Visel A, Mundlos S. 2015. Disruptions of Topological Chromatin Domains Cause Pathogenic Rewiring of Gene-Enhancer Interactions. *Cell* **161**: 1012–1025.

Maddalo D, Manchado E, Concepcion CP, Bonetti C, Vidigal JA, Han Y, Ogrodowski P, Crippa A, Rekhtman N, Stanchina E De, et al. 2014. In vivo engineering of oncogenic chromosomal rearrangements with the CRISPR/Cas9 system Danilo. *Nature* **516**.

Mali P, Yang L, Esvelt KM, Aach J, Guell M, DiCarlo JE, Norville JE, George M. Church. 2013. RNA-Guided Human Genome Engineering via Cas9. *Science* **339**: 823–827.

Mandal PK, Ferreira MR, Collins R, Meissner TB, Boutwell CL, Rossi DJ, Cowan CA, Ferreira LMR. 2014. Efficient Ablation of Genes in Human Hematopoietic Stem and Effector Cells using CRISPR/Cas9. *Cell Stem Cell* **15**: 643–652. http://dx.doi.org/10.1016/j.stem.2014.10.004.

Mangeot PE, Risson V, Fusil F, Marnef A, Laurent E, Blin J, Mournetas V, Massouridès E, Sohier TJM, Corbin A, et al. 2019. Genome editing in primary cells and in vivo using viral-derived Nanoblades loaded with Cas9-sgRNA ribonucleoproteins. *Nat Commun* **10**: 1–15. http://dx.doi.org/10.1038/s41467-018-07845-z.

Mao Z, Bozzella M, Seluanov A, Gorbunova V. 2008. Comparison of nonhomologous end joining and homologous recombination in human cells. *DNA Repair (Amst)* **7**: 1765–1771.

Maruyama T, Dougan SK, Truttmann MC, Bilate AM, Ingram JR, Ploegh HL. 2015. Increasing the efficiency of precise genome editing with CrIsPr-Cas9 by inhibition of nonhomologous end joining. *Nat Biotechnol* **33**: 1–9.

Meyers RM, Bryan JG, McFarland JM, Weir BA, Sizemore AE, Xu H, Dharia N V., Montgomery PG, Cowley GS, Pantel S, et al. 2017. Computational correction of copy number effect improves specificity of CRISPR-Cas9 essentiality screens in cancer cells. *Nat Genet* **49**: 1779–1784.

Miyaoka Y, Berman JR, Cooper SB, Mayerl SJ, Chan AH, Zhang B, Karlin-neumann GA, Conklin BR.

2016. Systematic quantification of HDR and NHEJ reveals effects of locus, nuclease, and cell type on genome- editing. *Sci Rep* 1–12. http://dx.doi.org/10.1038/srep23549.

Mochizuki Y, Chiba T, Kataoka K, Yamashita S, Sato T, Kato T. 2018. Combinatorial CRISPR/Cas9 Approach to Elucidate a Far-Upstream Enhancer Complex for Tissue- Specific Sox9 Expression. *Dev Cell* **46**: 794-806.e6. https://doi.org/10.1016/j.devcel.2018.07.024.

Mohiuddin IS, Kang MH. 2019. DNA-PK as an Emerging Therapeutic Target in Cancer. **9**: 1–8.

Nelson CE, Hakim CH, Ousterout DG, Thakore PI, Moreb EA, Rivera RMC, Madhavan S, Pan X, Ran FA, Yan WX, et al. 2016. In vivo genome editing improves muscle function in a mouse model of Duchenne muscular dystrophy. **351**: 403–408.

Pulido-Quetglas C, Aparicio-Prat E, Arnan C, Polidori T, Hermoso T, Palumbo E, Ponomarenko J, Guigo R, Johnson R. 2017. Scalable Design of Paired CRISPR Guide RNAs for Genomic Deletion. *PLOS Comput Biol* **13**: e1005341. http://dx.doi.org/10.1371/journal.pcbi.1005341.

Rene D, Greger JG, Katz RA, Taganov KD, Wu X, Kappes JC, Skalka AM. 2004. Evidence that Stable Retroviral Transduction and Cell Survival following DNA Integration Depend on Components of the Nonhomologous End Joining Repair Pathway. *J Virol* **78**: 8573–8581.

Riesenberg S, Chintalapati M, Macak D, Kanis P. 2019. Simultaneous precise editing of multiple genes in human cells. *Nucleic Acids Res* **47**.

Riesenberg S, Maricic T. 2018. Targeting repair pathways with small molecules increases precise genome editing in pluripotent stem cells. *Nat Commun* **9**: 1–9. http://dx.doi.org/10.1038/s41467-018-04609-7.

Robert F, Barbeau M, Éthier S, Dostie J, Pelletier J. 2015. Pharmacological inhibition of DNA-PK stimulates Cas9-mediated genome editing. *Genome Med* 1–11. http://dx.doi.org/10.1186/s13073-015-0215-6.

Sanson KR, Hanna RE, Hegde M, Donovan KF, Strand C, Sullender ME, Vaimberg EW, Goodale A, Root DE, Piccioni F, et al. 2018. Optimized libraries for CRISPR-Cas9 genetic screens with multiple modalities. *Nat Commun* **9**: 5416. http://www.nature.com/articles/s41467-018-07901-8 (Accessed May 15, 2019).

Schmittgen TD, Livak KJ. 2008. Analyzing real-time PCR data by the comparative CT method. *Nat Protoc* **3**: 1101–1108.

Song J, Yang D, Xu J, Zhu T, Chen YE, Zhang J. 2016. RS-1 enhances CRISPR/Cas9- and TALEN-mediated knock-in efficiency. *Nat Commun* **7**.

Stojic L, Lun ATLL, Mangei J, Mascalchi P, Quarantotti V, Barr AR, Bakal C, Marioni JC, Gergely F, Odom DT. 2018. Specificity of RNAi, LNA and CRISPRi as loss-of-function methods in transcriptional analysis. *Nucleic Acids Res* **46**: 5950–5966. http://www.ncbi.nlm.nih.gov/pubmed/29860520 (Accessed July 29, 2018).

Thomas JD, Polaski JT, Feng Q, De Neef EJ, Hoppe ER, McSharry M V, Pangallo J, Gabel AM, Belleville AE, Watson J, et al. 2020. RNA isoform screens uncover the essentiality and tumor-suppressor activity of ultraconserved poison exons. *Nat Genet* **52**. http://www.ncbi.nlm.nih.gov/pubmed/31911676.

Thul PJ, Åkesson L, Wiking M, Mahdessian D, Geladaki A, Ait Blal H, Alm T, Asplund A, Björk L, Breckels LM, et al. 2017. A subcellular map of the human proteome. *Science (80-)* **356**: eaal3321. http://www.ncbi.nlm.nih.gov/pubmed/28495876 (Accessed March 11, 2018).

Tsherniak A, Vazquez F, Montgomery PG, Weir BA, Kryukov G, Cowley GS, Gill S, Harrington WF, Pantel S, Krill-Burger JM, et al. 2017. Defining a Cancer Dependency Map. *Cell* **170**: 564-576.e16. http://dx.doi.org/10.1016/j.cell.2017.06.010.

Vidigal JA, Ventura A. 2015. Rapid and efficient one-step generation of paired gRNA CRISPR-Cas9 libraries. *Nat Commun* **6**: 1–7.

Xing Y-H, Yao R-W, Zhang Y, Guo C-J, Jiang S, Xu G, Dong R, Yang L, Chen L-L. 2017. SLERT Regulates DDX21 Rings Associated with Pol I Transcription. *Cell* **169**: 664-670.e16. http://dx.doi.org/10.1016/j.cell.2017.04.011.

Yang H, Wang H, Shivalila CS, Cheng AW, Shi L, Jaenisch R. 2013. One-Step Generation of Mice Carrying Reporter and Conditional Alleles by CRISPR/Cas-MediatedGenome Engineering. *Cell* **154**: 1370–1379. http://dx.doi.org/10.1016/j.cell.2013.08.022.

Yeh CD, Richardson CD, Corn JE. 2019. Advances in genome editing through control of DNA repair pathways. *Nat Cell Biol* **21**. http://dx.doi.org/10.1038/s41556-019-0425-z.

Zenke FT, Zimmermann A, Sirrenberg C, Dahmen H, Vassilev L, Pehl U, Fuchss T, Blaukat A. 2016. Abstract 1658: M3814, a novel investigational DNA-PK inhibitor: enhancing the effect of fractionated radiotherapy leading to complete regression of tumors in mice. In *Proceedingsof the*

108thAnnual Meeting of theAmericanAssociation for CancerResearch.

Zhu S, Li W, Liu J, Chen C-H, Liao Q, Xu P, Xu H, Xiao T, Cao Z, Peng J, et al. 2016. Genome-scale deletion screening of human long non-coding RNAs using a paired-guide RNA CRISPR–Cas9 library. *Nat Biotechnol* **34**: 1279–1286. http://www.nature.com/doifinder/10.1038/nbt.3715 (Accessed December 21, 2016).